A First Principle Study of Mechanical Strength of Kevlar-29

Harsha Verma[1] Jitendra Chauhan[2]
[1,2]Department of Mechanical Engineering
[1,2]Bhilai Institute of Technology, Durg, Chhattisgarh, India

Abstract— The first principle study is performed for the analysis of the mechanical strength of Kevlar-29. The structure is optimized by the density functional theory implemented in SIESTA. The bond strength is investigated by the displacement of central nitrogen atom along X, Y and Z directions; respectively. The structural property analysis provides an asymmetric nature of Kevlar-29. Larger bond breaking energy is observed during compression along Z direction and vice versa for elongation. There is strong s-p hybridization in the orbitals and exhibits an insulating nature. The forbidden energy gap is increased while compression and it reduces gradually during elongation. The bonds have higher ionic and lower covalent nature, there is larger covalency for applied strain along Z-axis, hence the strength is little higher along the same axis than along X and Y-axes. Larger stress is required along Z-axis to produce the strain and smaller along Y-axis, therefore; Kevlar-29 is mechanically stronger along its Z-axis and weaker along Y-axis.

Key words: SIESTA; Density functional theory; DOS; Tensile stress

I. INTRODUCTION

For the first time Kevlar was obtained in 1964 by the research team Stephanie Kwolek [1]. A production technology has been finalized a year later. In the study of synthetic features of fiber, Kevlar (Poly para-phenylene terephtalamide (PPTA)) is an important practice today; it is formed by combining para-phenylene diamine & terephthaloyl chloride [2-5]. It is a highly crystalline poly-aramid fiber with exceptionally high strength and remarkable thermal stability, widely used in stress-bearing applications such as bulletproof body armor, shielding for sports equipment and fiber-reinforced polymer composites in the aerospace industry [6-8]. Kevlar fiber has been extensively used in the fields of aerospace, military, marine or mountaineering etc, due to its good mechanical properties, thermal stability and energy absorption properties [9-10]. Kevlar is an example of an elastic polymer fibre with a high elastic modulus, a high breaking stress and a low breaking strain, it is several times stronger than steel [11-13].

Materials such as glass, carbon and Kevlar have extremely high tensile and compressive strength, and Kevlar have high strength, high modulus, toughness, and thermal stability [14,15], but in solid form, many random surface flaws are present in such materials, which cause them to crack and fail at a much lower stress.

II. METHODOLOGY

Simulation is performed by using a computational program SIESTA (Spanish Initiative for Electronic Simulations with Thousands of Atoms) based on a density-functional theory [16,17]. For exchange and correlation potential; a Generalized Gradient Approximation (GGA) of Perdew-Burke-Ernzerhof is used [18]. Core electrons are modeled with Troullier-Martins norm-conserving pseudopotentials [19] and the valence electrons functions are expanded in double zeta polarized basis set (DZP) [20,21] of localized orbitals and the real space grid is set to be 300 Ry. The structure is relaxed until the Hellmann-Feynman forces acting in all components of each atom are smaller than 0.01 eV/Å.

III. RESULTS AND DISCUSSION

The Equilibrium configurations of (Kevlar-29), (Kevlar-29)-x, (Kevlar-29)-y, (Kevlar-29)-z are shown in Figs. 1a,b,c & d, Where x, y and z are representing the variation in the displacement of central N-atomic position till to respective bond is broken along X,Y and Z axis, respectively. There is a little variation in the bond lengths between C and Central atom N of a Kevlar-29 (K-29) during 10% displacement of lattice constants along Y and Z axes, the C-N bond is broken for the elongation along X and Z axes and not along Y axis, hence; it exhibits an asymmetric nature of Kevlar-29.

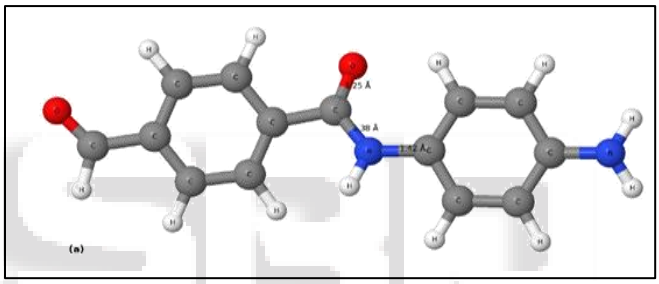

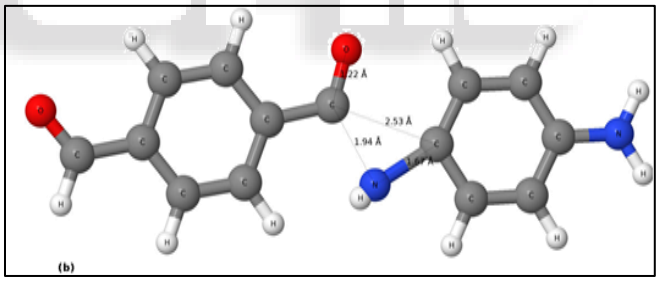

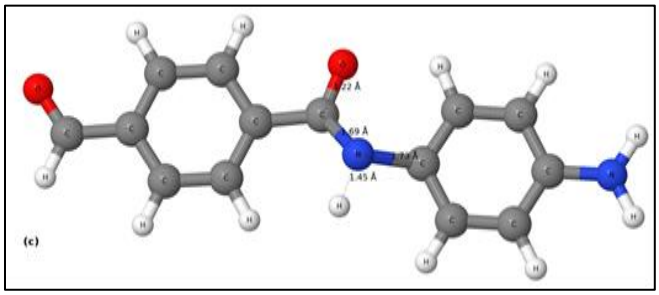

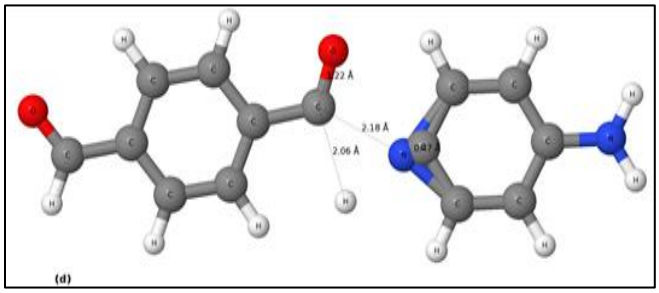

Fig. 1: Equilibrium Configurations of: a) Kevlar-29, b) Kevlar-29-x, c) Kevlar-29-y and d) Kevlar-29-z, where x, y, and z Representing the Breaking of Structure during the Variation of Central N-atomic Position along X,Y, and Z axis, Respectively.

To know the bond strength, the bond breaking energies of Kevlar-29 are calculated; during bond (C-N) compression/elongation along X, Y and Z axes and tabulated in Table 1. There is larger compression energy required to break the bond along Z-axis; it is 194.584 eV and smaller along Y-axis; it is 15.562 eV. During elongation of a bond; there is larger energy is required along X-axis; it is 18.703 eV and smaller along Z-axis; it is 1.219 eV. Hence, to break a bond (C-N); there is larger bond breaking energy required along Z-axis for compression and smaller energy during elongation. There is an analogy with our previous work [22]

Kevlar-29		(Kevlar-29)-x	(Kevlar-29)-y	(Kevlar-29)-z
Bond breaking energy in eV (when bond length of C-N is compressed/enlarged from its equilibrium position)	During compression	44.810	15.562	194.584
	During elongation	18.703	4.557	1.219

Table 1: C-N Bond Breaking Energy

In the projected density (PDOS) of states of Kevlar-29 (shown in Fig. 2a), 0 eV represents the Fermi level, s-orbitals are only contributing the lower valence and in higher conduction bands. In the higher valence band and in the lower conduction bands only p-orbital energy states are taking part in the density of states, amongst all p-orbitals, there is large contribution of p-orbitals of carbon C and oxygen O atoms and there is strong s-p hybridization among orbitals. In the forbidden energy gap, there are few p-orbitals of carbon C, nitrogen N and oxygen O found which reduces the crystalline nature of the system.

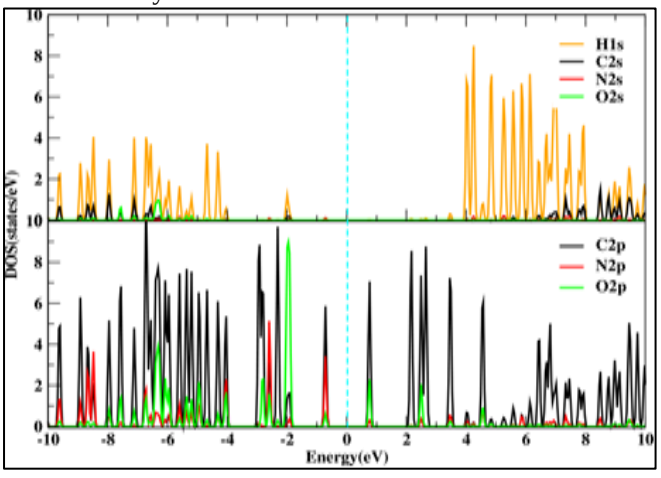

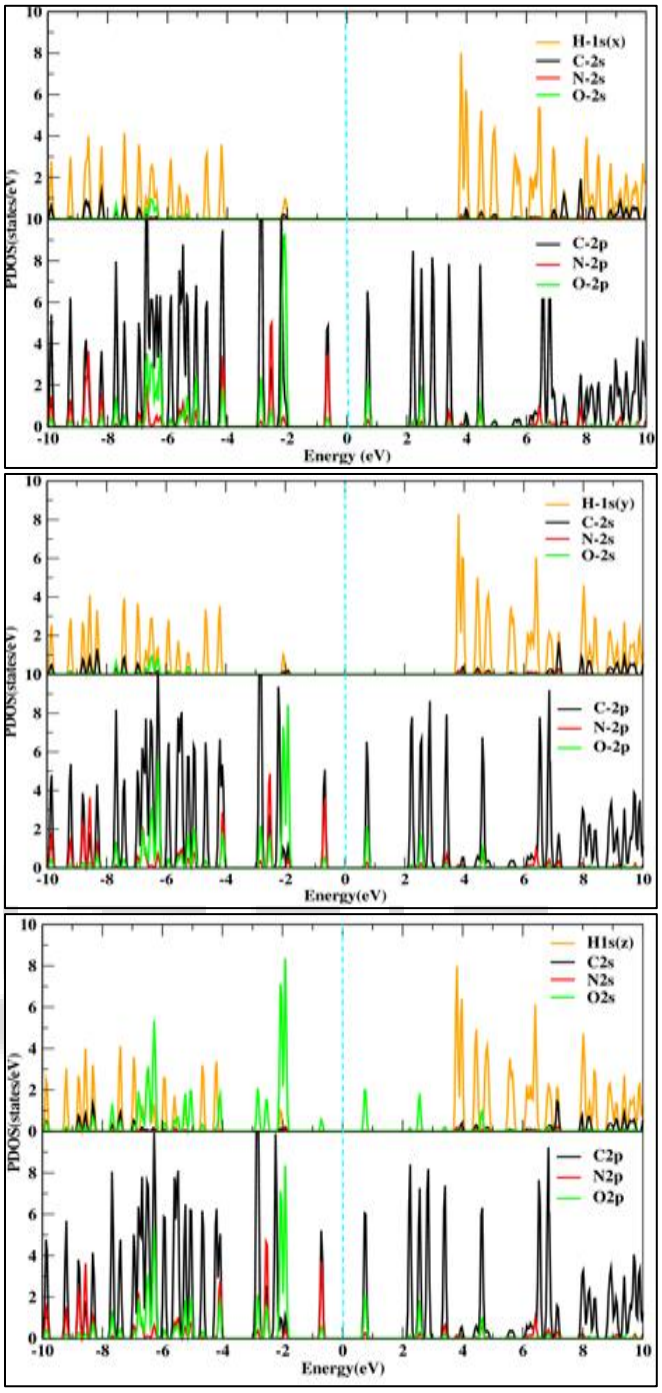

Fig. 2: PDOS of: a) Kevlar-29, b) Kevlar-29-x, c) Kevlar-29-y and d) Kevlar-29-z, where x, y, and z representing Equilibrium configurations for the variation of central N-atomic position along X, Y, and Z axis, respectively

If strain is applied along X and Y axes, there is little variation in the forbidden energy gap and in the distribution of orbital states (shown in Figs. 2b & c), but; the contribution of orbital states are similar as Fig. 2a. For strain along Z-axis, s-orbitals of oxygen O atoms are also contributing highly, and the remaining are same as mentioned above, it is shown in Fig. 2d.

In the density of states (DOS) analysis of Kevlar-29, the higher occupied energy state of valance band is at around -1.85 eV, lowest unoccupied energy state is at around 2.1 eV and the forbidden energy gap (Eg) is around 3.95 eV (it is

shown in Fig 3), it gives the insulating nature of Kevlar-29. 0 eV represents the Fermi energy. If strain is applied along all axes respectively, there is little change in the forbidden energy gap, it is 4.25 eV for X-axis, 4.0 eV for Y-axis and 4.0 eV for Z-axis, which can be observed in Fig. 3 and all values of Eg and Fermi energies are also tabulated in Table 2. By applying strain; Eg is increased, and there is larger change along X-axis. Few energy states are found in the forbidden region, just below and at higher energy states of Fermi level, which take part in the reduction of the crystallinity and increase in the amorphicity of K-29.

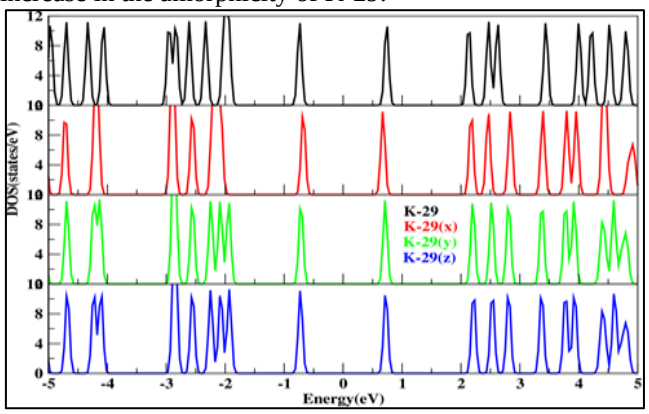

Fig. 3: DOS at equilibrium positions of Kevlar-29, Kevlar-29-x, Kevlar-29-y and Kevlar-29-z, where x, y, and z are representing the strain applied along X, Y and Z axis, respectively

System	Kevlar-29	(Kevlar-29)-x	(Kevlar-29)-y	(Kevlar-29)-z
Fermi energy (eV)	-4.263	-4.342	-4.339	-4.344
Forbidden energy gap (eV) (± 5%)	3.950	4.250	4.000	4.000

Table 2: Fermi Energy and Forbidden Energy Gap of Systems

The tensile stress is calculated by applying strain along X, Y & Z axes by following the equation [23]:

$$\sigma = (1/\Omega(\varepsilon))\ \partial E/\partial \varepsilon \ldots\ldots\ldots\ldots\ldots\ldots(1)$$

Where, σ be the tensile stress, E be the total energy and Ω(ε) be the volume at given strain (ε). All calculated values are tabulated in Table 3, the negative values of strain and tensile stress are representing the compression and positive values for elongation of C-N bond of Kevlar-29. The results of compression are approximately equal to the experimental values [24] along X and Y

Strain applied along the axis	Strain	Tensile Stress in GPa	Experimental Values in GPa [24]
X-axis	-0.013	−0.223	-0.185
	0.047	1.460	1.850
	0.077	2.230	
Y-axis	-0.040	−0.181	-0.185
	0.070	0.377	1.850
	0.100	0.509	
Z-axis	-0.041	−2.253	-
	0.018	1.099	-
	0.048	2.657	-

Table 3: Tensile Stress And Strain along the Axes axes. For elongation; the calculated values along X axis are nearly equal to the experimental value, but for Y axis these are too smaller. Due to unavailability of experiment values along Z-axis, stress values couldn't be compared. But it is comparable to the experimental values of K-29 irrelevant of axes [25].

According to the tabulated values, it can be said that there is higher tensile stress required during elongation of a bond than compression; it is around 10 times higher along X-axis and 2-3 times along Y-axis. Along Z-axis higher tensile stress is required for compression than the first value of strain of elongation, and approximately equal for second value of strain.

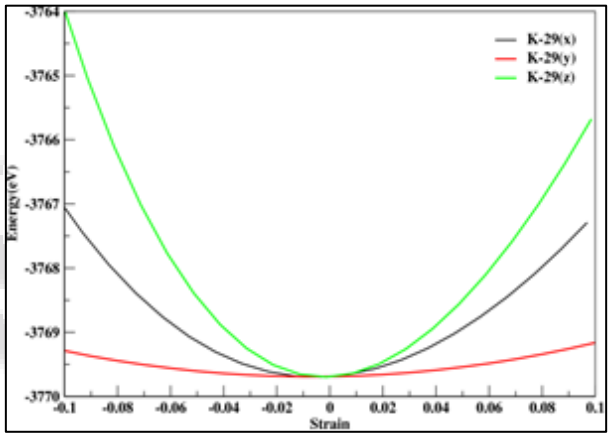

Fig. 4: Energy vs. Strain along X, Y and Z Axes

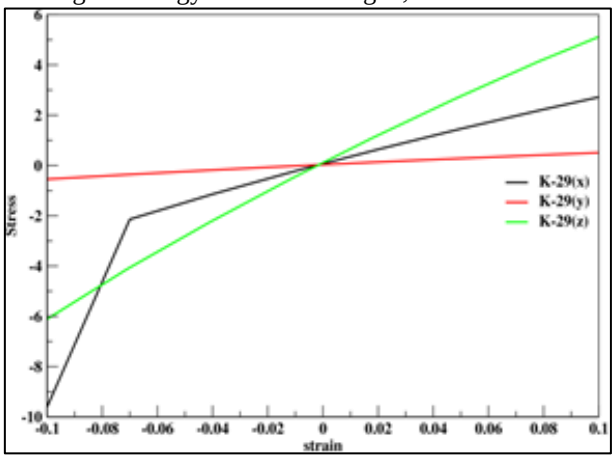

Fig. 5: Stress vs. Strain along X, Y and Z Axes

The analysis of total energy of Kevlar-29 with respect to strain is shown in Fig. 4, it explains that the total energy of a system is increased during compression as well as elongation for all axes. To produce same strain; the ration of increasing of energy is higher along Z-axis and lower along Y-axis. Fig. 5 explains the linear relation between stress and strain for all axes, to produced same strain; larger stress is

required to apply along Z-axis and smaller along Y-axis, i.e. Kevlar-29 is mechanically stronger along its Z-axis and of weaker strength along Y-axis.

IV. CONCLUSIONS

The structural property analysis exhibits an asymmetric nature of Kevlar-29. There is required of larger bond breaking energy along Z-axis during compression of C-N bond, and vice versa for elongation. PDOS explains the strong s-p hybridization among orbitals and DOS for an insulating nature of K-29. At equilibrium condition, while applying strain; the forbidden energy gap is increased, it is larger along X-axis.

There is higher ionic and lower covalent nature of bonds of K-29, there is larger covalency between the atoms for applied strain along Z-axis, hence the strength is little higher along the same axis than X & Y-axes. Larger stress is required to apply along Z-axis to produce the strain and smaller along Y-axis, i.e. K-29 is mechanically stronger along its Z-axis and weaker along Y-axis.

ACKNOWLEDGMENTS

We gratefully acknowledge the kind support of the Department of Mechanical Engineering, BIT, Durg.

REFERENCES

[1] N. Hancox, Materials and Design, 14 (1993) 312-313.
[2] H.H. Yang, Kevlar aramid fiber, New York, John Wiley & Sons, 1993.
[3] J.K. Fink, High performance polymers, William Andrew, 2008.
[4] J.W. Downing, J.A. Newell, J. Applied Polymer Science, 91 (2004) 417-424.
[5] G.O. Phillips, M. Takigami, T. Hongu, New millennium fibers, USA: Woodhead Publishing, 2005.
[6] S.N. Raja, S. Basu, A.M. Limaye, T.J. Andersone, C.M. Hyland, L. Lin, A.P. Alivisatos, R.O. Ritchie, doi.org/10.1016/j.mtcomm, 2014.
[7] B.D. Agarwal, L.J. Broutman, K. Chandrashekhara, Analysis and Performance of Fiber Composites, third ed., Wiley Publication, 2006.
[8] T.T. Li, R. Wang, C.W. Lou, J.H. Lin, Compos. Part B Eng. 59 (2014) 60-6.
[9] T.J. Singh, S. Samanta, 2 (2015) 1381-1387.
[10] A.K. Bandaru, V.V. Chavan, S. Ahmad, R. Alagirusamy, N. Bhatnagar, I. J. Impact Engineering, 79 (2016)136-143.
[11] F.J. Wortmann, K.V. Schulz, 36 (1995) 2363-2369.
[12] A. Pregoretti, M. Traina, A. R. Bunsell (Eds.), Handbook of Tensile Properties of Textile and Technical Fibers, Woodhead Publishing Limited, Cambridge, (2009) 354–436.
[13] R.J. Young, D. Lu, R.J. Day, W.F. Knoff, H.A. Davis, J. Mater. Sci. 27 (1992) 5431–5440.
[14] A.A. Leal, J.M. Deitzel, S.H. McKnight, J.W. Gillespie Jr., 50 (2009) 1228-1235.
[15] F. Guo, Z. Zhang, W.M. Liu, F.H. Su, H.J. Zhang, 42 (2009) 243-249.
[16] P. Hohenberg and W. Kohn, In homogeneous electron gas, Phys. Rev. 136 (1964) B864-71.
[17] M. Solar et al. The SIESTA method for ab initio order-N materials, J. Phys: Condens Matter, 14 (2002) 2745.
[18] J.P. Perdew, K. Burke, M. Ernzerhof, Phys. Rev. Lett. 77 (1996) 3865.
[19] N. Trouillier, J.L. Martins, Phys. Rev. B. 43 (1991) 1993.
[20] J. Junquera, O. Paz, D.S. Portal, E. Artacho, Phys. Rev. B. 64 (2001) 235111.
[21] C. Shen, J. Wang, Z. Tang, H. Wang, H. Lian, J. Zhang, C. Cao, Electrochim. Acta, 54 (2009) 3490.
[22] M.L. Verma, B.K. Rao, R. Singh, D. Banchor and H.D. Sahu, J. Ionics, (2017) DOI 10.1007/s11581-017-2025-x.
[23] L.Y. Lin, Z. Ying, H.R. Jie, L.G. Hong, Chinese Physics B, 18 (2009) 1923.
[24] L.M. Bresciani, A. Manes, A. Ruggiero, G. Iannitti, M. Giglio, Composite Part B, 88 (2016) 114-130.
[25] 25. D. Ahmed, Z. Hongpeng, K. Haijuan, L. Jing, M. Yua, Y. Muhuo, Materials Research, 17 (2014) 1180-1200.

